Comparison of Channel Estimation Methods for DAB Systems in a Multipath Fading Channels[1]

JAEKYOUNG MOON[2]

†Sensor Technology Research Center
School of Electrical Eng. and Computer Science
Kyungpook National University
1370 Sankyuk-dong, Buk-gu, Daegu 702-701, Republic of Korea

(Communicated by Y.H. Sohn)

Abstract

In this paper, a Gaussian interpolation filter and cubic interpolation filter are presented to do more accurate channel estimation compared to the conventional linear interpolation filter for DAB systems. In addition to an interpolation filter, a low pass filter using FFT and IFFT is also presented to reduce the noisy components of a channel estimate obtained by an interpolation filter. Channel estimates after low-pass filtering combined with interpolation filters can lower the error floor compared to the use of only interpolation filters. Computer simulation demonstrates that the presented channel estimation methods exhibit an improved performance compared to the conventional linear interpolation filter for DAB systems in time-varying multipath fading channel and $0.1 \sim 0.2$ dB of E_b/N_o difference at $BER = 10^{-4}$ when the perfect channel estimation is compared.

Keywords: Gaussian interpolation filter, Cubic interpolation filter, DAB systems.

1 Introduction

Recently, there has been considerable interest in using Orthogonal Frequency Division Multiplexing (OFDM) systems for wireless transmission, such as in Digital Audio Broadcasting (DAB) and Digital Video Broadcassting (DVB).

OFDM allows the overlapping of adjacent frequency subchannels or subcarriers with orthogonality between them. The spectrum of each subchannel is zero on the other subcarrier frequencies. Therefore, it is a great advantage that the OFDM transmitter and receiver can be implemented using efficient fast Fourier transform (FFT) techniques. An OFDM system also requires channel estimation in its time-varying multipath fading channels although this is less complex than in single carrier systems.

---

1) Accepted 5 November 2005.

2) E-mail: jkmoon@ee.knu.ac.kr.

The reliable detection of an OFDM signal in time-varying multipath fading channels is a challenging problem. Various channel estimation methods have been proposed for performance improvement. One way of estimating a channel is to multiplex pilots (known symbols) into the transmitted signal. All channel attenuations are estimated from these symbols using an interpolation filter. This technique is called pilot symbol assisted modulation (PSAM) and has been originally introduced for single carrier systems [3].

In this paper, a Gaussian interpolation filter and cubic interpolation filter are presented as more accurate interpolation filters compared to the conventional linear interpolation filter. However, despite an increased signal to noise ratio (SNR), the presented interpolation filters also suffer from an error floor, that is an irreducible bit error rate (BER). The mean squared error (MSE) of the channel estimations produced by the three interpolation filters is analyzed using computer simulations. In addition to an interpolation filter, a low pass filter using FFT and IFFT is also presented to reduce the noisy components of a channel estimate obtained by an interpolation filter. A channel estimate is first transformed into a time domain and low-pass filtered. The values are then transformed back into a frequency domain in order to obtain the final channel estimate. Channel estimates after low-pass filtering combined with interpolation filters can lower the error floor compared to the use of only interpolation filters. Computer simulation demonstrates that the presented channel estimation methods exhibit an improved performance compared to the conventional linear interpolation filter. This is due to the combined use of an interpolation filter and low pass filter plus there is a reduced complexity compared to the optimal Wiener filter [7]. In this paper, a digital audio broadcasting (DAB) system parameter as an application area for an OFDM system and channel models suitable to a DAB system in their frequency modulation (FM) band are applied to the computer simulation [11,12]. The computer simulations are performed to evaluate the performance of the presented channel estimators for an OFDM system.

This paper is organized as follows: In Section 2, concept of OFDM system, configuration of Coded-OFDM DAB system and selection of pilot pattern are discussed. The presented channel estimation methods are described in Section 3. Simulation results are presented in Section 4, and conclusions are drawn in Section 5.

2   System Model

2.1   Concept of the OFDM System

The symbols to be transmitted are fed into a serial-to-parallel converter and then an inverse fast Fourier transform, IFFT, is performed. The samples from the IFFT are then converted to a serial form, extended by a cyclic prefix, mixed to an appropriate frequency, and the transmitted over the radio channel. Mathematically speaking: The linear convolution performed by the channel is transferred into a cyclic convolution, which, after the FFT, behaves like a scalar multiplication using a channel transfer function [1]:

$$r(k) = x(k) \otimes h(k) + n(k) \tag{1}$$

where $x(k)$ is the data sequence, $h(k)$ is the channel impulse response, and $R(l)$ is the received vector at the FFT input. The FFT output coefficients $R(l)$ are, therefore, equal to:

$$R(l) = H_m(l)X(l) + N(l), \;\; 0 \leq l \leq N-1, \tag{2}$$

where $N(l)$ is the zero-mean complex-Gaussian independent random variable representing AWGN and $H_m(l)$ are thus the complex-valued variables representing the multipath channel:

$$H_m(l) = \sum_{h=0}^{N-1} h_m(k)e^{-j2\pi \frac{lk}{N}}, \;\; 0 \leq l \leq N-1. \tag{3}$$

These symbols are assumed to be independent, identically distributed, and possibly coded. A serial-to-parallel converter transfers blocks of symbols to the OFDM modulator, which then uses an N-point IFFT to modulate them onto the subchannels. The set $\{a(n), 0 \leq n \leq N-1\}$ is the set of symbols to be modulated. Then the N-point IFFT output is

$$x(k) = \sum_{n=0}^{N-1} a_i(n)e^{j2\pi nk/N}, \;\; 0 \leq k \leq N-1. \tag{4}$$

The set, $\{x(k), 0 \leq k \leq N-1\}$, corresponds to the samples at $t = kT$ of $\bar{x}(t)$, the sum of the subcarrier signals, expressed as

$$\bar{x}(t) = \frac{1}{\sqrt{N}} \sum_{n=0}^{N-1} a(n)e^{j2\pi nt/NT}, \;\; 0 \leq t \leq NT, \tag{5}$$

where $T_u = NT$ is the block period.

To reduce the ISI between the blocks, the guard interval of length G which consists of $\{x(N-G), x(N-G+1), \cdots, x(-1)\}$ can be appended to the beginning of the block. The addition of a guard interval increases the length of one block sequence from N to $(N+G)$ samples, which may be indexed as $k = -G, \cdots, N-1$. The sequence after adding the guard interval is written as

$$x^g(k) = \frac{1}{\sqrt{N}} \sum_{n=0}^{N-1} a(n)e^{j2\pi nk/N}, \;\; -G \leq k \leq N-1. \tag{6}$$

The first g elements of (6) constitute the guard samples. In practice, the sequence $x^g(k)$ is passed through a D/A converter whose output would ideally be the signal waveform $\bar{x}^g(t)$:

$$\bar{x}^g(t) = \frac{1}{\sqrt{N}} \sum_{n=0}^{N-1} a(n)e^{j2\pi nt/NT}, \;\; -GT \leq t \leq NT, \tag{7}$$

where $T_s = (N+G)T = T_u + T_G$ and $T_G = GT$ is the guard interval.

It is the IFFT that transforms the signals so that the samples from the serial-to-parallel converter constitute a signal where the data is transmitted on several subcarriers. All of the values from one IFFT constitute samples from one OFDM symbol. Therefore, the symbol time for the OFDM symbol is M times longer than the symbol time for the data symbols, where M is the number of points in the IFFT. In this way it is possible to extend the OFDM symbol time, and make it much longer than the maximum excess delay, thereby making the echoes affect only the first part of the next symbol, but no more.

A demodulator removes a guard interval according to $r(k) = r^g(G + (k - G)_N)$, $0 \leq k \leq N-1$, and performs an FFT on the resulting sequence. It is assumed that a channel impulse response exists within a guard interval. Thus $x^g(k - m)$ for $k < m$ corresponds to a value within a guard interval, allowing for an independent analysis of the data blocks. The demodulated sequence can be written as

$$R(l) = \sum_{n=0}^{N-1} \sum_{m=0}^{M-1} a(n)H_m(n - l)e^{-j\frac{2\pi nm}{N}}, \quad 0 \leq l \leq N - 1, \tag{8}$$

where

$$H_m(n - 1) = \frac{1}{N} \sum_{k=0}^{N-1} h_m(G + (k - G)_N)e^{-j\frac{2\pi k}{N}(n-l)}.$$

The channel estimator is discussed in the following chapter.

2.2 Configuration of the Coded-OFDM DAB System

The baseband model of the pilot-based COFDM system is shown in Fig. 1. The data source generated a pseudo random binary sequence. The information bits were then error-protected by means of a convolutional encoder. After being bit-interleaved and symbol-interleavered (time and frequency interleaving), the bits were paired into 2 bits or 4 bits and mapped into QPSK or 16QAM by the individual subcarriers. After signal mapping, the pilot symbols are inserted. If N is the number of subcarriers; then the N encoded phases were grouped to form a complex vector of size N. This vector was multiplied by the power of 2 and applied to an IFFT which then performed the OFDM modulation. The guard interval was formed by a modulo extension which copied the last quarter of the symbol into its beginning. After being sent through the mobile channel, the guard interval of the received COFDM signal was removed and demodulated with an FFT. The data on each subcarrier was then compensated after estimating the channel frequency response. Following this channel estimation and compensation, the pilot symbols were removed and the signal was demapped. Plus the symbol and bit were deinterleavered. The output of the deinterleaver was quantized before being fed to the Viterbi decoder. The outputs of the decoder were then compared to the source data bits and finally the bit error rate (BER) was measured.

2.3 Selection of Pilot Pattern

The most important parameters for the selection of a pilot pattern are the expected maximum speed, which determines the minimum coherence time, and the maximum
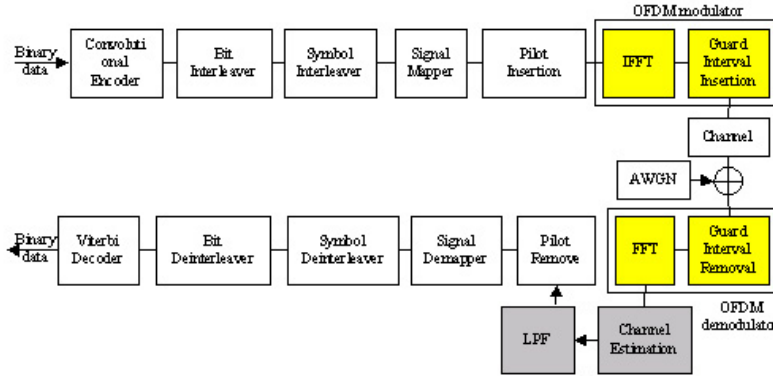
Figure 1: Baseband model of pilot-based COFDM system

excess delay, which determines the minimum coherence bandwidth. The pilot symbols should be placed close enough together to be able to follow the time and frequency variations of the transfer function, yet far enough apart so as not to increase the over-head too much. In order to accommodate all variations, the lower limit for the pilot density is determined using the Nyquist sampling theorem. In practice, however, the fading process is more often sampled in order to obtain reliable channel estimates for insertion as pilot symbols. In [7] it is suggested that twice as many pilot symbols in time and frequency are advisable when using the sampling theorem. A suitable choice of pilot spacing in time, N_T, and in frequency, N_F, is as follows:

$$N_T \approx \frac{1}{2}\frac{1}{2f_D T_{sub}}, \tag{9}$$

$$N_F \approx \frac{1}{2}\frac{1}{2\Delta f \tau_{max}}, \tag{10}$$

where Δf is the sub-carrier bandwidth, T_{sub} the symbol time, and τ_{max} the maximum excess delay of the channel. If a low complexity channel estimator is used, e.g. two 1-dimensional estimators instead of one 2-dimensional estimator, the system is extremely sensitive to the choice of the pilot density, however, the "two times the Nyquist frequency rule" seems to work well even in this case. The relation between time and frequency in pilot spacing is important to minimize pilot density. It is advantageous to have the same "uncertainty" in both time and frequency directions in order to achieve a "balanced" pilot pattern [7]. This can also be viewed as maintaining the same distance between the pilot symbols in both directions when normalized by the coherence bandwidth and time. If coherence time is defined as $1/f_D$ and coherence bandwidth is the inverse of the excess delay, $1/(\tau_Q(t) - \tau_I(t))$, then, according to expressions (9) and (10), a suitable pilot spacing is one fourth of the coherence time and coherence bandwidth, respectively. In practical situations channel characteristics are often unknown since, for example, it is preferable to avoid the requirement of measuring the Doppler frequency. For the simplicity and robustness of a channel estimator an adjustment according to the worst case scenario for the Doppler frequency and excess delay is often suggested, i.e. to the minimum correlation in time and fre-

quency. In general, adequate pilot symbols are inserted so as to follow any variations in time and frequency. As a result, pilot spacing is determined by the Doppler spectra and power delay profile for the whole system, including any hardware impairments such as oscillator drift and phase noise.

In this OFDM system, the number of subcarriers (N) is 512. The total bandwidth is 512kHz, thus the subcarrier spacing (Δf) is 1kHz and $T_{sub} = 1$ms. The maximum delay time (τ_{max}) is different according to the power delay profile. For example, in the worst case scenario, when τ_{max} is 50μs the pilot spacing in both the time and frequency directions is less than 5. By varying the channel model, it was found that when $N_T = 4$ and $N_F = 4$ this was close to optimal in terms of BER. The presented pilot pattern is shown in Fig. 2.
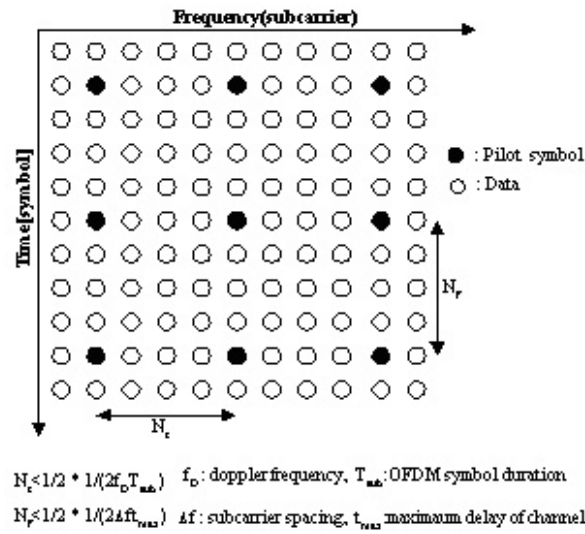

Figure 2: Pilot pattern in presented system

This means that the redundancy when using pilot symbols is $1/16$ (about 6%) of the bandwidth. This value is reasonable compared to 12.5% in the European DVB-T (digital video broadcasting-terrestrial) system. Moreover, the power of a transmitted pilot symbol is very important from a performance perspective. To further improve the performance of channel estimation, the pilot symbols can be boosted above the data carrier average power density. The performance by boosted pilot symbols is higher in 3dB compared to that by non-boosted pilot symbols. The corresponding pilot value is given by

$$\text{Re}(a_p) = 4/3 \times 2(w_k - 1/2), \ w_k = 0 \text{ or } 1,$$
$$\text{Im}(a_p) = 0 \tag{11}$$

where w_k is the value according to random number generation. Therefore, the value of a pilot symbol (a_p) is only a real value, $4/3$ or $-4/3$. The power of a boosted pilot symbol is higher in 3dB than that of a data symbol. The data values (a) are

normalized modulation values of constellation point (c). The normalization factors yield $E[aa^*] = 1$ and are shown in Table 1.

Table 1: Normalization factors for data symbols

Modulation scheme	Normalization factor
QPSK	$a = c/\sqrt{2}$
16QAM	$a = c/\sqrt{10}$

3   The Presented Channel Estimation Methods

Since 2-D filters tend to have a high computational complexity in the time and frequency directions, the outer product of two 1-D filters can offer a good trade-off between performance and complexity. Based on the selected pilot pattern, a 1-D filter is applied in the frequency direction. Thereafter, a 1-D filter is applied in the time direction to complete the interpolation to all points in the grid.

These two separate 1-D filters can be described as 2-D because the channel correlation is separable. This is given in the following equation. The auto-correlation of the channel model (12) is

$$
\begin{aligned}
R_{GG}(\Delta f, \Delta t) &= E\{H(f;t)H^*(f - \Delta f; t - \Delta t)\} \\
&= \left\{ \frac{1}{M} \sum_{n,n'=1}^{M} e^{j(\theta_n - \theta_{n'})} e^{j2\pi(F_{D,n}t - F_{D,n'}(t - \Delta t))} \right. \\
&\quad \left. \times e^{-j2\pi(f\tau_n - (f - \Delta f)\tau_{n'})} \right\}.
\end{aligned}
\tag{12}
$$

Since all random variables are independent, (12) is as follows:

$$
\begin{aligned}
R_{GG}(\Delta f, \Delta t) &= \frac{1}{M} \sum_{n=1}^{M} E\left\{e^{j2\pi F_{D,n}\Delta t}\right\} E\left\{e^{-j2\pi\Delta f\tau_n}\right\} \\
&= E\left\{e^{j2\pi F_{D,n}\Delta t}\right\} E\left\{e^{-j2\pi\Delta f\tau_n}\right\} = R_f(\Delta f)R_t(\Delta t),
\end{aligned}
\tag{13}
$$

i.e., the channel correlation is separable. The expectations can be found from a standard Fourier transform such that

$$
R_t(\Delta t) = E\left\{e^{j2\pi F_{D,n}\Delta t}\right\} = J_0(2\pi F_{D,max}\Delta t),
\tag{14}
$$

$$
R_f(\Delta f) = E\left\{e^{j2\pi\Delta f\tau_n}\right\} = \frac{(1 - e^{-T_{cp}(1/\tau_{rms} + j2\pi\Delta f)})}{(1 - e^{-T_{cp}/\tau_{rms}})(1 + j2\pi\Delta f\tau_{rms})},
\tag{15}
$$

where $J_0(\cdot)$ is the zeroth order Bessel function of the first kind.
Note that the correlation function for a uniform power-delay profile can be obtained

by letting $\tau_{rms} \to \infty$ as follows:

$$R_f^{uniform}(\Delta f) = E\left\{e^{j2\pi F_{D,n}\Delta t}\right\} = \frac{1 - e^{-j2\pi\Delta f T_{cp}}}{j2\pi\Delta f T_{cp}}. \tag{16}$$

The correlation between channel attenuations separated by k subcarriers and l OFDM symbols is

$$E\left\{h_{k',l'}h^*_{k'-k,l'-l}\right\} = r_f(k)r_l(k), \tag{17}$$

where

$$
\begin{aligned}
r_f(k) &= R_f\left(\frac{k}{NT_s}\right) = \frac{1 - e^{-L(1/\tilde{\tau}_{rms}+j2\pi k/N)}}{(1 - e^{-L/\tilde{\tau}_{rms}})(1 + j2\pi k\tilde{\tau}_{rms}/N)}, \\
r_t(l) &= R_t(l(N+L)T_s) = J_0\left(2\pi f D, \max(1 + \frac{L}{N})l\right),
\end{aligned}
$$

and $\tilde{\tau}_{rms} = \tau_{rms}/T_s$ is the RMS-spread relative to the sampling interval.

Suppose there is a memory to save N_T consecutive OFDM symbols containing pilot symbols, then the demodulated OFDM symbol can be written as follows:

$$Y(l,k) = H(l,k)X(l,k) + N(l,k), \tag{18}$$

where l is the frequency gain index ranging between 0 and $N-1$ and k ranges between 1 and the sample size of N_T which can be adjusted.

The channel attenuations at pilot positions are denoted by

$$
\begin{aligned}
\tilde{H}_p(l,k) &= \frac{Y_p(l,k)}{X_p(l,k)} = \frac{H_p(l,k)X_p(l,k) + N(l,k)}{X_p(l,k)}, \\
&= H_p(l,k) + \frac{N(l,k)}{X_p(l,k)}
\end{aligned}
\tag{19}
$$

where $Y_p(l,k)$ is the signal received at the subcarrier l by the OFDM symbol k and $X_p(l,k)$ is the corresponding transmitted pilot symbol. The final estimates of the channel attenuations $H(l,k)$ at the data positions are linear combinations of $H_p(l,k)$, where the coefficients are chosen according to the structure of each estimator.

Conventional channel estimation uses a linear interpolation filter. Since this linear interpolation filter only requires two pilot symbols per estimate, this method is very effective in a practice sense. The gain and phase of a channel is estimated in frequency as follows:

$$\tilde{H}(l + \frac{m}{N_f}, k) = (1 - \frac{m}{N_f})\tilde{H}_p(l,k) + m\tilde{H}_p(l+1,k) \tag{20}$$

where N_f is the pilot spacing in the frequency direction and m is from 1 to $N_f - 1$. $\tilde{H}_p(l,k)$ is the channel estimate of a pilot symbol at position l in frequency and k in time, and $\tilde{H}_p(l_1,k)$ at position $l+1$ in frequency and k in time. Thereafter, the gain and phase of a channel can be estimated in time as follows:

$$\tilde{H}(l, k + \frac{n}{N_t}) = (1 - \frac{n}{N_t})\tilde{H}_p(l,k) + n\tilde{H}_p(l,k+1) \tag{21}$$

where N_t is the pilot spacing in the time direction and n is from 1 to $N_t - 1$, and $\tilde{H}_p(l, k+1)$ is at position 1 in frequency and $k+1$ in time.

However, one disadvantage is that the estimation accuracy is slightly decreased. A more accurate interpolation filter is, therefore, needed, yet it should not be more complex than the existing linear interpolation filter. Accordingly, this paper presents two interpolation filters, a Gaussian interpolation filter and a cubic spline interpolation filter for use in OFDM systems.
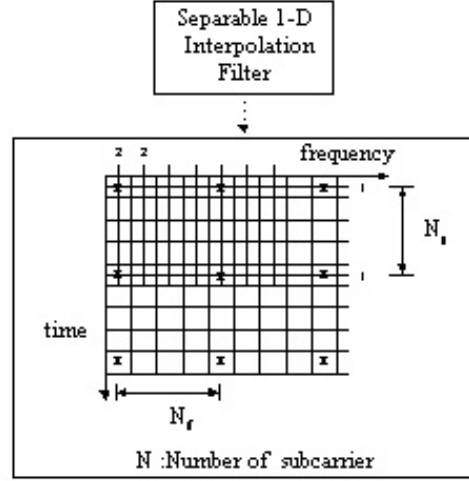

Figure 3: The presented Separate 1-D Interpolation filter

3.1   Gaussian Interpolation Filter

Fig. 3 illustrates the structure of channel estimation using separable 1-D PSAM (Pilot Symbol Assisted Modulation: PSAM). Based on the pilot pattern proposing a four spacing of time and frequency, a separable 1-D 2nd Gaussian Interpolation Filter (GIF) is first applied in the frequency direction [4]. Thereafter, a separable 1-D 1st GIF is applied in the time direction to complete the interpolation to all data points. The amounts in the block box in Fig. 3 must be stored in order to exploit the correlation in the time and frequency directions.

The 1-D 2nd GIF is as follows:

$$\tilde{H}(l + \frac{m}{N_f}, k) = Q_{-1}(m/N_f)\tilde{H}_p(l-1, k) + Q_0(m/N_f)\tilde{H}_p(l, k)$$

$$+Q_1(m/N_f)\tilde{H}_p(l+1, k), \tag{22}$$

$$Q_{-1}(m/N_f) = \frac{1}{2}\left\{(m/N_f)^2 - (m/N_f)\right\},$$

$$Q_0(m/N_f) = 1 - (m/N_f)^2, \tag{23}$$

$$Q_1(m/N_f) = \frac{1}{2}\left\{(m/N_f)^2 + (m/N_f)\right\},$$

where $\tilde{H}_p(l + m/N_f, k)$, which is a channel estimate at position $l + m/N_f$ in frequency and k in time, is calculated based on three channel estimates of the previous, present, and next pilot symbol. $\tilde{H}_p(l - 1, k)$ is a channel estimate of the previous pilot symbol at position $l - 1$ in frequency and k in time, $\tilde{H}_p(l, k)$ at position l in frequency and k in time, and $\tilde{H}_p(l + 1, k)$ at position $l + 1$ in frequency and k in time. The channel estimation for the first four data symbols of the 1st OFDM symbol is thus obtained using two pilot symbols. A processing delay occurs due to the consideration of the next pilot symbol. Linear interpolation is the same. N_f is the pilot spacing of the frequency direction and m is from 1 to $N_f - 1$.

Thereafter, a channel estimate in time is obtained as follows:

$$
\begin{aligned}
\tilde{H}(l, k + \frac{n}{N_t}) &= Q_{-1}(n/N_t)\tilde{H}_p(l, k - 1) + Q_0(n/N_t)\tilde{H}_p(l, k) \\
&\quad + Q_1(n/N_t)\tilde{H}_p(l, k + 1), \\
Q_{-1}(n/N_t) &= 0, \\
Q_0(n/N_t) &= 1 - \frac{n}{N_t}, \\
Q_1(n/N_t) &= \frac{n}{N_t},
\end{aligned}
$$

(24)

(25)

where $\tilde{H}_p(l, k + n/N_t)$, which is a channel estimate of at position l in frequency and $k + n/N_t$ in time, is calculated based on two channel estimates of the present and next pilot symbol. $\tilde{H}_p(l, k)$ is a channel estimate of the present pilot symbol at position l in frequency and k in time, and $\tilde{H}_p(l, k + 1)$ at position l in frequency and $k + 1$ in time. A processing delay occurs due to the consideration of the next pilot symbol in the time direction. The presented channel estimation method only requires a memory of $N \times N_t$, where N is the number of subcarriers and N_t is the pilot spacing in the time direction.

Due to the use of a 1st order interpolation in time, only two pilot symbols are used per estimate, therefore, a 1st order Gaussian interpolation is the same as a linear interpolation.

3.2   Cubic Spline Interpolation Filter

The second interpolation filter presented is a cubic spline interpolation filter (CSIF). This filter is used in the frequency direction instead of a 2nd Gaussian interpolation filter (GIF). In this case, the application of a 1st GIF for an interpolation in time is as same as in the first presented scheme. In Fig. 3, a 1-D CSIF is applied in the frequency direction first and then a 1-D 1st GIF is applied in the time direction.

Given N_s pilot points in one OFDM symbol, $N_s - 1$ polynomials are obtained. A channel estimate for the data symbols between the pilot symbols can be obtained using these polynomials.

3.3   Low Pass Filter

Errors caused by interpolation and noise are included in an estimated channel response through the use of an interpolation filter. Therefore, these estimators suffer
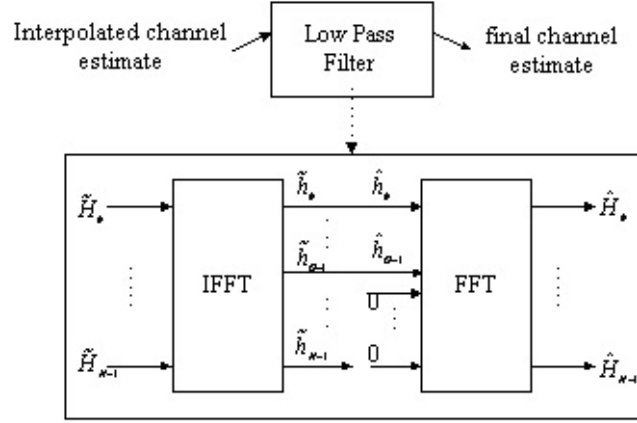
Figure 4: The presented low-pass filter using IFFT/FFT

from an error floor caused by these errors. In order to reduce this error floor, a low-pass filter (LPF) is combined with the presented interpolation filters. A low-pass filter plays the role of removing the noise components while preserving the channel impulse response. The maximum channel duration of a channel impulse response can be anticipated from the guard interval of the OFDM system. An LPF is implemented using IFFT/FFT modules as shown in Fig. 4.

After estimating the fading distortion due to the interpolation filter, this estimate is then transformed into the time domain using IFFT to obtain a transformed estimate. As a result, this transformed estimate can be regarded as the channel impulse response. In general, a guard interval is longer than the maximum delay time of a channel impulse response. Accordingly, it can be assumed that the channel impulse response, that is the most powerful multipath, is contained within the guard interval. The remainder outside the guard interval can be considered as noise components. Therefore, zero values instead of noise components are inserted for the IFFT processing. As a result, the original transformed estimate within the guard interval plus these zero values are then transformed once more in the frequency domain using FFT to obtain a final channel response estimate without noise components.

4   Experiments and Discussion

To ascertain the performance of the two presented channel estimators, a low-pass filter combined with a separable 1-D Gaussian interpolation filter and a separable 1-D cubic spline interpolation filter, the computer simulations were performed in time-varying multipath fading channels. A block diagram of the system model used for the analysis and simulation is shown in Fig. 1. The mean squared error (MSE) and coded bit error rate (BER) were adopted as the performance measures of the presented schemes.

4.1   Simulation Parameters

The feasibility of the application of the OFDM method to digital audio broadcasting (DAB) was investigated. In Europe, the Eureka-147 DAB system has been developed in a bandwidth of about 6MHz as a "new-band" system [13]. In contrast, since there are fewer available radio frequencies in the USA and Korea, a DAB system must operate within the existing FM band - carrier frequencies from 88 to 108MHz - as an "in-band" system [11].

Two different In-Band transmission modes, IBOC (In-Band On Channel) and IBAC (In-Band Adjacent channel) are available to accommodate transmission at RF frequencies ranging from 88MHz to 108MHz. The FM IBAC and IBOC DAB spectrum is shown in Fig. 5. IBAC means an adjacent channel whereas IBOC means on a channel within the FM band.

The simulation parameters suitable to a DAB system within the FM band are shown in Table 2. The transmission bandwidth was 512kHz and the modulation scheme used for each subcarrier was QPSK and 16QAM. The number of subcarriers and FFT size was 512. The carrier spacing was 1kHz and the useful symbol duration was a reciprocal of the carrier spacing. The guard interval was determined as $1/32$ of the useful symbol duration that included the maximum delay time of the channel impulse response. The total symbol duration then added the useful symbol duration to the guard interval. The total bit rate was about 512 kbps for QPSK and 1024 kbps for 16QAM.

Table 2: System parameters for COFDM system

Transmission bandwodth [kHz]	512
Modulation for each subcarrier	QPSK or 16QAM
Number of subcarriers	512
FFT size	512
Carrier spacing(kHz)	1
Useful symbol duration(μs)	1000
Guard interval(μs)	31.25 (1/32 of useful symbol duration)
Total symbol duration(μs)	1031.25
Total bit rates(kbps)	$512 \sim 1024$

The baseband model used for the analysis and simulation of the pilot-based OFDM system is shown in Fig. 2. For error correction, a $1/2$ rate convolutional code with the octal polynomial $(133, 171)$ was used, i.e., the code polynomials were

$$
\begin{aligned}
g_0^{(0)}(D) &= 1 + D + D^3 + D^4 + D^6, \\
g_0^{(1)}(D) &= 1 + D^3 + D^4 + D^5 + D^6.
\end{aligned}
\tag{26}
$$

The constraint length was $n_E = 7$ and a tail of $n_E + 1 = 8$ zeros was appended to

clear the encoder's memory. The receiver used a soft-decision Viterbi decoder with a truncated memory length of $5n_E = 35$bits.
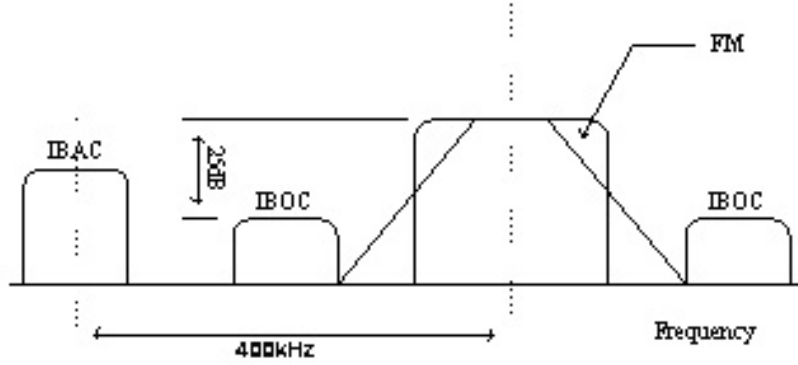

Figure 5: FM IBAC (In-Band Adjacent Channel) and IBOC (In-Band On-Channel) DAB Spectrum

4.2   Channel Model

The transmission media of the terrestrial broadcasting of the DAB signal were FM bands. A FM band spanning a frequency range of 88 MHz through 108 MHz is described here in terms of multipath fading and noise. The USADA (United States of America Digital Audio) models a selective-fading channel by summing a number of delayed and attenuated flat-faded Rayleigh paths. This fading model was applied in the FM simulations [11,12]. The multipath model was used: "urban fast(UF)". The "fast" modifier refer to the ground speed of the vehicle on which the receiver is mounted. This ground speed directly determines the degree of the Doppler spread experienced by the signal. The tap number of "urban fast" delay profile was 9 and the maximum delay time was 3μs. The Doppler frequency was 5.2314Hz for each path, with a speed of velocity at about 57km/h. These conditions represent a car that is driven fast in an urban environment. The relative time of the multipath and attenuation in each tap is shown in Table 3.

4.3   Simulation Results and Discussion

In order to evaluate the performance of the presented channel estimations, the mean squared error (MSE) was analyzed for a delay profile. Plus, the coded bit error rate (BER) was calculated.

4.3.1   Performance Results of Presented Methods from MSE

The performance of the presented channel estimators was evaluated from the perspective of the MSE. The MSE, that is, the average error over all the attenuations, can be expressed as:
$$MSE = |H(l,k) - \tilde{H}(l,k)|^2 \tag{27}$$

Table 3: Urban Fast Rayleigh Multipath Profile

Tap #	Relative Time (μs)	Attenuation (dB)
1	0.0	2.0
2	0.2	0.0
3	0.5	3.0
4	0.9	4.0
5	1.2	2.0
6	1.4	0.0
7	2.0	3.0
8	2.4	5.0
9	3.0	10.0

where $H(l, k)$ is the known channel frequency response and $\tilde{H}(l, k)$ is the estimated channel frequency response using the presented channel estimators.

The performance of the presented channel estimator was evaluated against that of a low-pass filter combined with a conventional linear interpolation filter. The relative performances were evaluated using simulation results from an urban-fast Rayleigh multipath fading profile:

- Conventional channel estimator: low-pass filter combined with separable 1-D linear interpolation filter.

- Presented channel estimator 1: low-pass filter combined with separable 1-D Gaussian interpolation filter.

- Presented channel estimator 2: low-pass filter combined with separable 1-D cubic spline interpolation filter / Gaussian interpolation filter.

- Pilot pattern : as shown in Fig. 3.

- Modulation : 16QAM.

- Delay profile : Urban-Fast Rayleigh Multipath profile.

In Fig. 6, the MSEs for the channel estimators are shown as a function of E_s/N_o. The upper-three channel estimators in Fig. 6 are a separable 1-D linear interpolation filter (LIF), separable 1-D Gaussian interpolation filter (GIF), and separable 1-D cubic spline interpolation filter (CSIF), respectively. The lower three channel estimators are the same as the upper three except for being combined with a low pass filter. The upper three channel estimators using only an interpolation filter had error floors at $E_s/N_o > 16$dB. When compared to each other, the E_s/N_o of the linear interpolation filter required 1.2dB more than the Gaussian interpolation filter and 1.7dB more than the cubic spline interpolation filter when MSE=10^{-2}. Therefore, of the three interpolation filters, the cubic spline interpolation filter is the best and the linear interpolation

filter the worst. However, since these three interpolation filters had an error floor at a high SNR, this needs to be reduced. To reduce an error floor, this paper has presented the addition of a low-pass filter (LPF). The error floors were lowered in the lower three channel estimators with the use of low-pass filters. It should be noted, however, that the mutual ordering was the same as for the upper channel estimators. Accordingly, a low-pass filter combined with a cubic spline interpolation filter was the best and a low-pass filter combined with a linear interpolation filter was the worst. The difference between a LPF combined with a CSIF and a LPF combined with a linear interpolation filter was about 3dB. In Fig. 6, it can be seen that interpolation filters performed better with LPFs than without them.
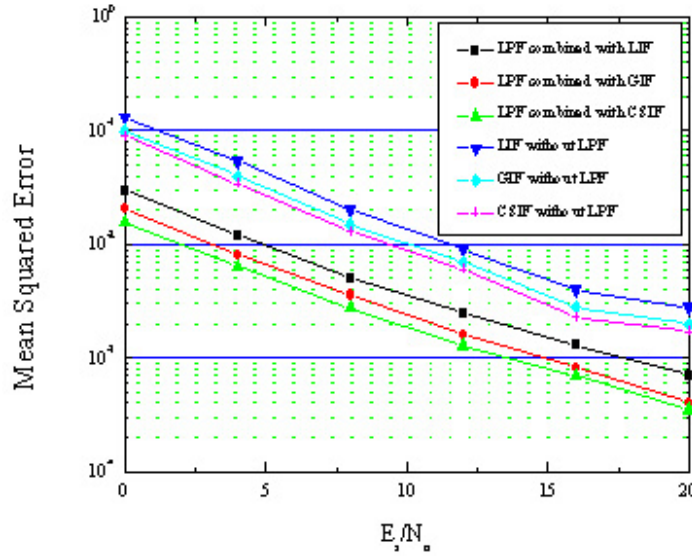

Figure 6: Mean squared error for three channel estimators in Urban Fast Rayleigh Multipath delay profile

4.3.2   Signal Constellation Before and After Channel Estimation

To establish the effect of channel estimation, signal constellations before and after channel estimation are shown in Fig. 7. These are shown as in-phase (I) on the X-axis and quadrature-phase (Q) on the Y-axis since the transmission signal is quite complex. The relative performance of the presented channel estimator for 16QAM can be seen from this figure. The 16QAM-signal constellation before channel estimation is shown in Fig. 7(a), whereas the 16QAM-signal constellation after channel estimation is shown in Fig. 7(b). The simulation conditions were as follows:

- Channel: urban-fast profile.

- Presented channel estimator 1: low-pass filter combined with separable 1-D Gaussian interpolation filter.

- E_s/N_o : 14dB.

In Fig 7(a), the signal constellation before channel estimation has been faded by a time-varying multipath fading channel. However, in Fig. 7(b) this faded signal has been nicely compensated by the presented channel estimator. In Fig. 7(b) an error floor is slightly visible caused by random dots beyond the decision boundary of the 16 point signal. Thus, there will always be an interpolation error, even in noiseless cases, as all estimators have an error floor due to finite filter lengths. Even though a low-pass filter is used to reduce the error floor, it can not remove it completely. However, these errors can be corrected with a Viterbi decoder.

4.3.3   Performance Comparison of Presented Channel Estimators with Conventional Channel Estimator

The performances of the presented channel estimators were compared to that of a conventional channel estimator. In contrast to the presented channel estimators, the conventional channel estimator used a linear interpolation filter (LIF) configured with a separable 1-D filter for time and frequency directions. The presented channel estimators employed a Gaussian interpolation filter (GIF) and cubic spline interpolation filter (CSIF). First, the BER performance of the interpolation filters was evaluated for the one channel model and modulation schemes, using QPSK and 16QAM. However, all channel estimators using interpolation filters included an error floor. Accordingly, this paper presents the addition of a low-pass filter to reduce this error floor. Secondly, the BER performance of the interpolation filters combined with LPFs was evaluated for each case. In addition, the conventional channel estimator using linear interpolation filter was also combined with a low-pass filter for comparison with the presented channel estimators. Finally, the BER performance for perfect channel estimation was compared to the presented channel estimators and conventional channel estimator. Perfect channel estimation exists when a receiver knows the channel perfectly. Depending on the type of audio materials transmitted, degradation starts to be audible at BER values ranging typically from 10^{-3} to 10^{-4} [15]. Thus, as a reference, a BER value of 10^{-4} was chosen. A time interleaving depth (TID) of 256ms was chosen by computer simulations.

In Fig. 8, coded BER performances are shown for channel estimators using interpolation filter and using an LPF combined with an interpolation filter in an urban-fast profile. In this profile the Doppler frequency was 5.2314Hz and the maximum delay time 3μs. For QPSK, in Fig. 8(a), when comparing the BER performance of the channel estimators using an interpolation filter, the conventional channel estimator required about $0.3 \sim 0.5$dB more than the presented GIF and CSIF channels. The GIF in the presented channel estimator required about 0.2dB more than the CSIF. From this result, it can be seen that the CSIF is the best since it considers the most pilot symbols, whereas the linear interpolation filter is the worst because it considers only two pilot symbols. For 16QAM, in Fig. 8(b), the conventional linear interpolation filter required about $0.3 \sim 0.5$dB more than the presented GIF and CSIF channels. The difference between the GIF and CSIF was the same as for QPSK.

However, when compared to symbol duration (1ms), there was no substantial degradation in performance relative to interpolation type with a small delay time ($3\mu s$) in the multipath fading channel.

Secondly, for QPSK, the performance gain from using an LPF was about 1.2dB for the conventional linear interpolation filter and about $1 \sim 1.1$dB for the presented GIF and CSIF interpolation filters. For 16QAM, the performance gain from using an LPF was about 1.5dB for the conventional linear interpolation filter and about $1.2 \sim 1.3$dB for the presented GIF and CSIF interpolation filters. Therefore, it is clear that an LPF can effectively remove an error floor caused by an interpolation filter. As a result, a substantial performance gain can be obtained when a low-pass filter is combined with an interpolation filter.

Finally, when compared to perfect channel estimation for QPSK, the performance of an LPF combined with the CSIF required about 0.1dB more, that of an LPF combined with the GIF required about 0.2dB more, and that of an LPF combined with the linear interpolation filter required about 0.5dB more.

For 16QAM, when compared to perfect channel estimation, the performance of an LPF combined with the CSIF required about 0.1dB more, that of an LPF combined with the GIF required about 0.2dB more, and that of an LPF combined with the linear interpolation filter required about 0.4dB more. The BER will decrease with an increased complexity the closer it gets to perfect channel estimation.

### 4.3.4   Complexity Comparison

To evaluate the relative complexities of conventional channel estimation with the presented channel estimation, the complexities of the different interpolation filters can be compared based on the number of pilots they use. The conventional linear interpolation filter uses only two pilot symbols. In contrast, the presented Gaussian interpolation filter uses three pilot symbols. Thus, the difference between the conventional linear interpolation filter and the GIF is only one pilot symbol. Accordingly, the presented GIF can improve performance by about 0.3dB without any substantial increase in complexity. The cubic spline interpolation filter uses all the pilots within one OFDM symbol to estimate the channel of an OFDM symbol plus the polynomials between pilots must also be calculated. Therefore, the CSIF is the most complicated compared to the other two interpolation filters. From a performance perspective, the CSIF exhibited an improved performance of about 0.5dB compared to the conventional linear interpolation filter. All three interpolation filters have the same amount of memory due to exploiting the correlation in the time and frequency directions. Consequently, there has to be a trade-off between complexity and accuracy of estimation.

5   Conclusions

This paper describes the channel estimation methods using a low-pass filter combined with a Gaussian interpolation filter and cubic spline interpolation filter based
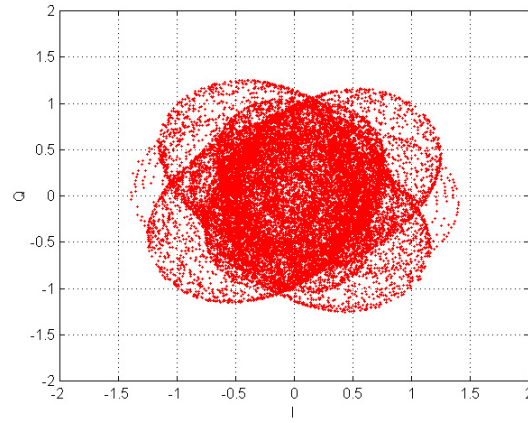
(a)
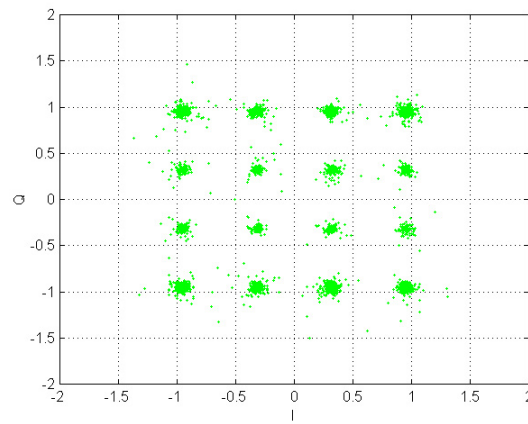
(b)

Figure 7: (a) Signal constellation before channel estimation for 16QAM, (b) Signal constellation after channel estimation for 16QAM

on PSAM (Pilot symbol Assisted Modulation). As with a conventional linear interpolation filter, the channel estimators using the presented interpolation filters also suffered from an error floor, apparently due to interpolation. Therefore, a low-pass filter using FFT and IFFT is also presented. This LPF preserves the channel impulse response while removing the noise components. As a result, channel estimation using a low-pass filter combined with an interpolation filter can decrease the error floor and be implemented in an OFDM system using a small amount of storage and FFT/IFFT modules.

Although a linear interpolation filter has the lowest complexity, from a mean squared error (MSE) perspective it is the worst method. In addition, when compared with the presented channel estimators under the same conditions, the conventional linear interpolation filter applies a separable linear interpolation filter in the time and
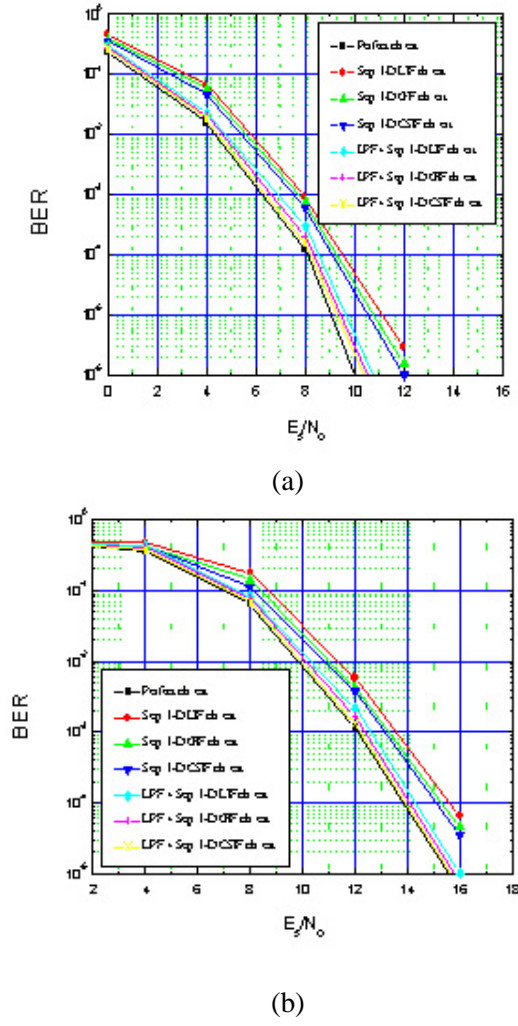
(a)

(b)

Figure 8: (a) BER performance for QPSK in urban-fast profile, (b) BER performance for 16QAM in urban-fast profile

frequency directions, thereby requiring the same amount of memory as the presented channel estimators: that is $N \times N_t$, where N is the number of subcarriers and N_t is the pilot spacing in the time direction.

The presented low-pass filter enhances performance by lowering the error floor caused by interpolation. An LPF combined with a conventional linear interpolation filter produces an improvement of about 1.2dB compared to without an LPF. Furthermore, the presented LPF combined with a GIF and CSIF produce an improvement of about $1 \sim 1.1$dB compared to without an LPF. Therefore, it is clear that a low-pass filter plays an important role in lowering an error floor and the combination with a low-pass filter is better than the use of an interpolation filter alone. Finally, when compared to perfect channel estimation, the performance of an LPF combined with the CSIF requires about 0.1dB more, that of an LPF combined with the GIF requires

about 0.2dB more, and that of an LPF combined with the linear interpolation filter requires about 0.5dB more. Accordingly, for perfect channel estimation, a combination of the presented LPF with the interpolation filters produced a 0.3dB gain compared to an LPF combined with a conventional linear interpolation filter. Consequently, the presented channel estimators using a low-pass filter plus interpolation filters exhibited an improved performance without a substantial increase in complexity.

Digital audio broadcasting (DAB) system parameters, as the application area of the OFDM system, and channel models suitable to a DAB system in their frequency modulation (FM) band were applied to a computer simulation. The simulation results of this DAB system can be used as a performance measure for comparison with other DAB systems with the same frequency band.

References

[1] L. Thibault and M. Thien Le, "Performance evaluation of COFDM for digital audio broadcasting Part I: Parametric study," *IEEE Trans. Broadcasting*, Vol. 43, pp.64-75, 1997.

[2] S.B. Weinstein and P.M. Ebert, "Data transmission by frequency-division multiplexing using the discrete Fourier transform," *IEEE Trans. Communication*, Vol. COM-19, pp. 628-634, 1971.

[3] J.K. Cavers, "An analysis of pilot symbol assisted modulation for Rayleigh fading channels," *IEEE Trans. Vehicular Technology*, Vol. 40, pp. 686-693. 1991.

[4] S. Sampei and T. Sunaga, "Rayleigh fading compensation method for 16QAM in digital land mobile radio channels," *Proc. of IEEE 39th Vehicular Technology Conference*, pp. 640-646, May 1989.

[5] L.J. Cimini, Jr., "Analysis and simulation of a digital mobile channel using orthogonal frequency division multiplexing," *IEEE Trans. Communication*, Vol. COM-33, pp. 665-675, 1985.

[6] J. Rinne and M. Renfors, "Pilot spacing in orthogonal frequency division multiplexing systems on practical channels," *IEEE Trans. Consumer Electronics*, Vol. 42, pp.959-962, 1996

[7] M. Sandell and O. Edfors, "A comparative study of pilot-based channel estimators for wireless OFDM," Div. of Signal Processing, Lulea Univ. of Technology, Lulea, Sweden, Tech. Rep. Sep. 1996.

[8] M. Russell, and G.L. Stuber, "Interchannel interference analysis of OFDM in a mobile environment," *Proc. of IEEE 45th Vehicular Technology Conference*, pp. 820-824, July 1995.

[9] M. Han Hsieh and C. H. Wei, "Channel estimation for OFDM systems based on comb-type pilot arrangement if frequency selective fading channels," *IEEE Trans. Consumer Electronics*, Vol. 44, pp. 217-225, 1998.

[10] Y. Zhao, A. Huang, "A novel channel estimation method for OFDM mobile communication systems based on pilot signals and Transform-domain processing," *Proc. of IEEE 47th Vehicular Technology Conference*, Phoenix, AZ, USA, pp. 2089-2093, May 1997.

[11] "Petition for rulemaking to the United States Federal Communications Commission for in-band on channel digital audio broadcasting," USA Digital Radio, Oct. 7,1998.

[12] L. Thibault, G. Soulodre and T. Grusec, "EIA/NRSC DAR systems subjective tests Part II: Transmission impairments," *IEEE Trans. Broadcasting*, Vol. 43, pp.353-364, 1997.

[13] "Radio Broadcasting System; Digital Audio Broadcasting (DAB) to Mobile, Portable, and Fixed Receivers," European Telecommunication Standard, ETS 300 401, June 1996.

[14] "Digital Broadcasting Systems for Television, Sound and Data Services," European Telecommun. Standards Institute, ETS 300 744, Valbonne, France, 1996.

[15] T. Grusec and L. Thibault, "MUSICAM Listening Tests Report," Commun. Research Centre, Ottawa, Canada, CRC Rep. CRC-RP-91.001, 1991.